IEEE Access
Multidisciplinary | Rapid Review | Open Access Journal

Received January 9, 2019, accepted January 30, 2019, date of publication February 4, 2019, date of current version February 22, 2019.

Digital Object Identifier 10.1109/ACCESS.2019.2897290

On the Design of Broadband Hybrid Amplifiers Using Non-Uniform Transmission Lines as Impedance Matching Networks

MIGUEL FERNÁNDEZ, SAMUEL VER HOEYE, (Member, IEEE), CARLOS VÁZQUEZ, LETICIA ALONSO, (Student Member, IEEE), AND FERNANDO LAS-HERAS, (Senior Member, IEEE)

Department of Electrical Engineering, University of Oviedo, E33203 Gijón, Spain

Corresponding author: Miguel Fernández (fernandezgmiguel@uniovi.es)

This work was supported in part by the European Union Seventh Framework Programme (FP/2007-2013) under Project 600849, in part by the Spanish Agencia Estatal de Investigación (AEI) and Fondo Europeo de Desarrollo Regional (FEDER) under Project TEC2016-80815-P (AEI/FEDER, EU) and Project TEC2015-72110-EXP (AEI), and in part by the Gobierno del Principado de Asturias (PCTI/FEDER-FSE) under Project IDI/2016/000372 and Project IDI/2017/000083.

ABSTRACT In this paper, an approach for the practical design of broadband amplifiers in hybrid technology is presented. It is based on the use of non-uniform transmission lines to implement impedance matching networks, which are synthesized exploiting the powerful optimization tools available in the most common computer-aided design software packages. The versatility of the proposed technique makes it suitable for the design of a wide variety of broadband amplifiers. Furthermore, it is easily implementable in most microwave simulators and allows a considerable design time reduction, since it can be applied in a systematic way and avoids the use of external tools. To validate the technique, it is applied to the design of a low noise amplifier using a single encapsulated transistor. A prototype was implemented, providing 10-dB flat gain from 1 to 12 GHz, noise figure under 2.5 dB, and acceptable input and output matching, which agrees with the simulation data.

INDEX TERMS Broadband amplifiers, impedance matching, non-uniform transmission lines, hybrid integrated circuits, circuit optimization.

I. INTRODUCTION

The design of broadband amplifiers working in the microwave and millimeter wave frequency bands has been widely treated during the last decades. On the one hand, Low Noise Amplifiers (LNA) are usually based on distributed topologies including several feedback transistors in which RLC networks are used to flatten their frequency response and to provide adequate impedance terminations [1]–[7]. Although these techniques provide very good results regarding the gain flatness, noise figure and impedance matching, they are only suitable in MMIC implementations. Furthermore, there is a great number of applications in which the custom design of the receiver front-end stage is required to limit the noise power, to facilitate the integration with the following stages, or to reduce the system cost, among many other causes. In that case, the LNA design usually comprises encapsulated transistors and input and output matching networks, which strongly conditions its performance.

On the other hand, considering Power Amplifiers (PA), they usually include broadband ladder impedance matching networks [8]–[14], which are obtained by interconnecting several transmission line sections with different characteristic impedance in the lowest microwave frequency band, or using transmission line segments connected with bond wires at higher frequencies. This approach presents some practical problems. In the first case, the radiation from the discontinuities may cause parasitic coupling and unwanted feedback phenomena, with an impact on the circuit stability. In addition, in the latter case, there is not a systematic design procedure, but it is usually based on the designer know-how.

This work presents an approach to design custom broadband amplifiers in hybrid technology, using discrete transistors. The proposed technique is based on the use of

The associate editor coordinating the review of this manuscript and approving it for publication was Bora Onat.

well-known Non-Uniform Transmission Lines (NUTL) to implement the required broadband impedance matching networks, and exploits the powerful optimization techniques available on the most common CAD packages. During the last years, a number of works describing analytical methods [15] to synthesize NUTL based broadband impedance matching networks [16], [17], ultra wideband filters [18], electromagnetic bandgap structures [19], and pulse shaping devices [20] with applications in medical imaging [21], have been presented. Despite the good reported results, the main drawbacks of these techniques are the necessity of the in-house implementation of the synthesis algorithm, the restriction of the line shape variation imposed by the considered method and the fact that, when using the resulting structures as a part of a more complex circuit, a global optimization of the system using CAD tools is still required.

On the other hand, to partially overcome the previously cited disadvantages, the possibility of directly synthesizing NUTL structures together with the circuit in which they are included, has also been described in the technical literature, with applications in the design of multi-harmonic DC-bias networks [22], [23], and in the optimization of multi-functional circuits based on harmonic [24], synchronized [25]–[28] and high efficiency [29], [30] oscillators. References [22]–[30] show that the key feature of the NUTL structures is the possibility of accurately controlling their input impedance over a relatively large frequency range located around different frequency points, which provides high design flexibility. In this way, the reported structures should be considered as multi-band instead broadband networks. From a practical point of view, the direct synthesis of the NUTL structures together the rest of the circuit considerably reduces the design time and complexity.

To demonstrate the viability of using NUTL based networks as practical broadband impedance matching networks, a broadband LNA which simultaneously provides 10 dB gain, noise figure less than 2.5 dB, and acceptable input and output impedance matching from 1 to 12 GHz was designed and implemented. First, the frequency dependent optimum impedance terminations are determined using the classical small signal approach. Next, the matching networks based on NUTL are synthesized in an optimization process which can be implemented in most commercial CAD software packages. Finally, a global optimization is carried out over the whole circuit. Due to its versatility and generalist character, the method can be easily extrapolated to be applied in the design of broadband power and multi-stage amplifiers, or adapted to other frequency limits, which will depend on the characteristics of the active device and on the suitability of using hybrid technology on the considered frequency range. To the best knowledge of the authors, this is the first time that NUTL structures synthesized through CAD optimization tools are used to design practical broadband amplifiers in hybrid technology.

The paper is organized as follows. In section II, the topology of the amplifier and the design method are described. Section III is devoted to the global optimization and fine tuning of the circuit using full wave methods. Finally, in sections IV and V, implementation aspects and experimental results are presented.

II. TOPOLOGY AND DESIGN

A. TOPOLOGY

The topology of the broadband LNA is schematized in Fig. 1. It is based on a single encapsulated ultra low noise pHEMT transistor. The Avago ATF36077 transistor was selected because it provides low noise figure in combination with moderate gain, and there is available a very good simulation model. The transistor works in common source mode and it is DC-biased with a drain voltage $V_d = 2$ V and gate voltage $V_g = -0.15$ V, which provides a drain current $I_d = 15$ mA. The DC-bias signals are connected to the transistor through two identical RF chokes, with an approximate inductance value $L_{\text{choke}} \approx 12$ nH and estimated self resonant frequency f_{SRF} above 14 GHz. A 50 Ω resistor R_{choke} is added in series with the gate RF choke for low frequency stabilization purposes. Another resistor $R_d = 20$ Ω is series connected with the transistor drain to improve the stability of the circuit. The reference planes at which the frequency dependent S parameters of the transistor are calculated are indicated in Fig. 1.

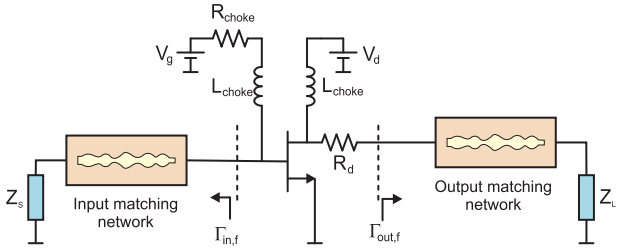

FIGURE 1. Topology of the amplifier. The reference planes at which the S parameters are evaluated are indicated with dashed lines.

B. CALCULATION OF THE OPTIMUM LOADS

In a first design step, the input and output optimum loads which simultaneously provide the required gain, noise figure, and input and output impedance matching, are selected using the conventional small signal approach [31]. They are defined in terms of their associated reflection coefficients $\Gamma_{in,f}$ and $\Gamma_{out,f}$, respectively, and calculated at discrete frequency points, covering the range between 3 and 13 GHz, with 2 GHz step.

The procedure is illustrated, at $f = 7$ GHz, in Figure 2. First, the output load $\Gamma_{out,7}$ over the power gain circle $G_p = 10$ dB was selected. Next, the circle containing the input impedance values set $\bar{\Gamma}_{in,7}(\Gamma_{out,7})$ that provide a maximum input voltage standing wave ratio $\text{VSWR}_{\text{in}} = 1.5$ when the output reference plane is loaded with the value of $\Gamma_{out,7}$ is calculated. Finally, the value of $\Gamma_{in,7}$ which provides minimum

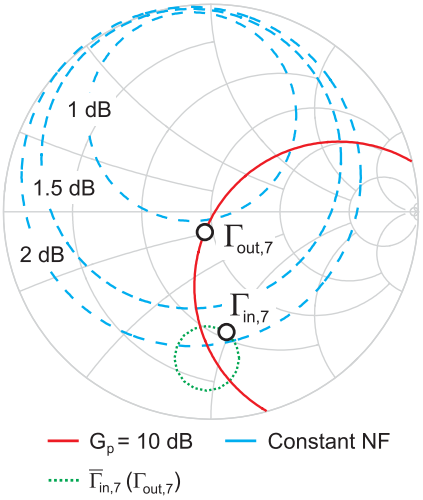

FIGURE 2. Selection of input $\Gamma_{in,7}$ and output $\Gamma_{out,7}$ reflection coefficients, at 7 GHz, as a trade off between gain, noise figure and input and output impedance matching.

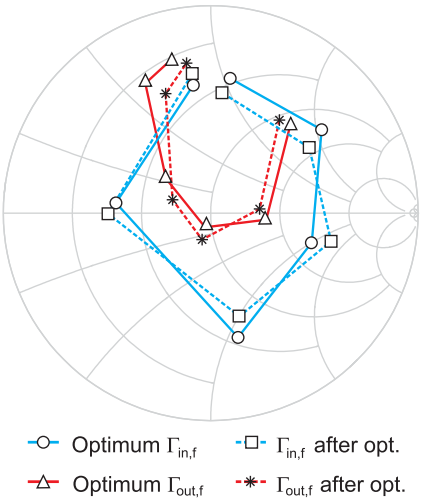

FIGURE 3. Set of selected input $\Gamma_{in,f}$ and output $\Gamma_{out,f}$ reflection coefficients, compared with those provided by the AWMML after the optimization process. The traces connecting the highlighted points do not represent valid values.

noise figure is selected over the previously calculated circle, and the amplifier output VSWR is estimated. The input and output stability circles are located around the border of the Smith Chart, due to the effect of the drain resistor, and they are not shown for the sake of the representation clarity. With the particular selection of $\Gamma_{out,7}$ and $\Gamma_{in,7}$ indicated in the figure, the amplifier is expected to provide a power gain $G_p = 10$ dB, noise figure $NF < 2$ dB, input $\text{VSWR}_{\text{in}} < 1.5$ ($S_{11} < -14$ dB) and $S_{22} < -10$ dB, at $f = 7$ GHz.

Note that the particular selection of $\Gamma_{in,f}$ and $\Gamma_{out,f}$ represents a trade-off between gain, noise figure, and input and output impedance matching of the amplifier. If it were not possible to meet the design specifications, the value of $\Gamma_{out,7}$ would have to be modified and the procedure repeated, or even the maximum value of VSWR_{in} increased.

In order to determine the frequency dependent behavior of the input and output matching networks, the described procedure is repeated for all the considered frequency points. The selected values of input and output reflection coefficients are shown in Fig. 3, at frequencies from 3 to 13 GHz, with 2 GHz step. The lines connecting the highlighted points do not represent valid values, but they help to understand the representation.

C. SYNTHESIS OF THE IMPEDANCE MATCHING NETWORKS

Once that the optimum reflection coefficients $\Gamma_{in,f}$ and $\Gamma_{out,f}$ at each considered frequency point are selected, the broadband matching networks based on NUTL can be synthesized. During the last years, some algorithms to obtain the width modulation function from the previously known frequency response [15]–[20] have been developed. However, in this work, a design approach directly implemented over the CAD software is used. The shape of the non-uniform transmission line is synthesized taking advantage of the powerful optimization tools available in most commercial microwave CAD software packages, avoiding the use of external in-house developed synthesis algorithms and, thus, increasing the flexibility of the method while reducing the design time.

The structure of the impedance matching networks, which can be seen as a transmission line whose width varies along its longitudinal direction, is shown in Fig. 4. The circuital implementation is composed of N trapezoidal shape short transmission line sections connected in series. In this work, $N = 150$ was selected. In the case of using microstrip transmission lines, most of commercial CAD software packages include an acceptable model of the trapezoidal shaped segment line. If other technologies are considered, or the model is not accurately implemented, it can be easily defined by the user, increasing in this way the versatility of the technique. Each base element is defined by its length ΔL, left hand side width W_i^l, and right hand side width W_i^r, with i the number of the element, varying from 1 to N. The left hand side width of each base element is forced to be equal to the right hand side width of the immediately previous one $W_i^l = W_{i-1}^r$, to ensure a smooth variation of the shape.

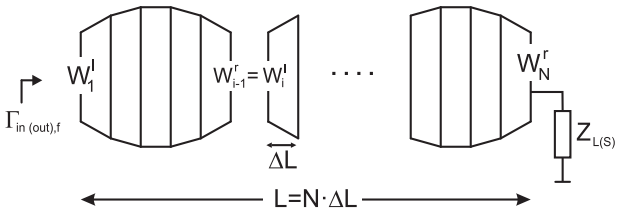

FIGURE 4. Structure of the Arbitrarily Width Modulated Microstrip Line and optimization setup.

To start the optimization process, all the elements are initialized with the same width. Thus, at this point,

a conventional transmission line with arbitrary length is obtained. One of its two terminals is loaded with the system reference impedance, usually $Z_{L(S)} = 50\ \Omega$. At the other terminal, the frequency dependent reflection coefficient $\Gamma_{in(out),f}$ is evaluated. The goal of the optimization process is to obtain a NUTL whose input reflection coefficient is equal to those calculated in the previous design step ($\Gamma_{in,f}$ or $\Gamma_{out,f}$, depending on which structure is being optimized), at the considered frequency points. The optimization variables are all the width parameters $\{W_i^r, W_i^l\}$, and ΔL. The parameter W_N^r is set equal to the width of a conventional transmission line with characteristic impedance $Z_o = 50\ \Omega$, and fixed. Figure 3 represents the frequency dependent input reflection coefficients $\Gamma_{in,f}$ and $\Gamma_{out,f}$ of the input and output matching networks, respectively, after the optimization process, together with the previously calculated goal values, showing very good agreement between them. The shape of the two matching networks is schematized in Fig. 5.

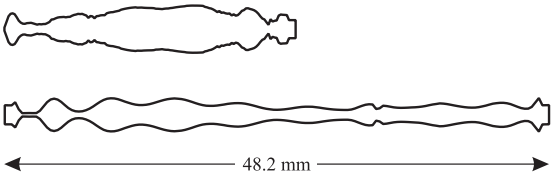

FIGURE 5. Shape of the input (below) and output (above) impedance matching networks after the optimization process. The left hand side terminal is the one connected to the corresponding transistor port.

III. AMPLIFIER GLOBAL OPTIMIZATION

After synthesizing the input and output matching networks, the frequency response of the whole amplifier was evaluated. The result is represented in Fig. 6, showing that the circuit meets the initial requirements only around the frequency points that were taken into account in the optimization process. Therefore, a second optimization step is required. In this case, the goals are expressed in terms of the S parameters of the amplifier:

$$\begin{cases} S_{11}(f) < -6\ (dB) \\ S_{22}(f) < -10\ (dB) \\ S_{21}(f) > 10\ (dB) \end{cases} \quad (1)$$

where f is evaluated at discrete points between 3 and 13 GHz, with 0.5 GHz step. Again, the optimization variables are the geometrical parameters that define the shape of the matching networks. The frequency response of the amplifier after this second optimization step is superimposed in Fig. 6, together with that obtained after the first one, which was performed over the two isolated matching networks. As can be observed, the goals expressed in (1) are satisfied and the circuit presents an acceptable performance in terms of stability, gain and input and output impedance matching.

A. FINE TUNING OF THE MATCHING NETWORKS

The circuital model of the short length trapezoidal transmission line segments implemented in the CAD software

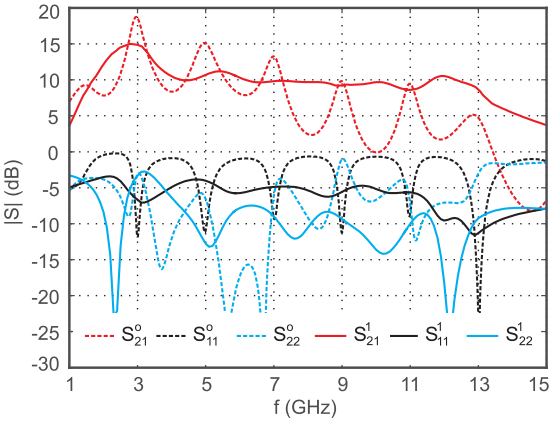

FIGURE 6. Frequency response of the amplifier after the global optimization (second step, superscript [1]), compared with that obtained after the optimization of the isolated matching networks (first step, superscript [o]).

packages provides a relatively good estimation of their behavior, but it does not take into account effects as the interconnection between them, or the electromagnetic coupling phenomena that can appear between sections of the same structure, depending on its shape. Therefore, despite the circuital model allows the direct and fast optimization of the NUTL, the effects which are not considered could have a negative impact on the circuit performance.

To solve this problem, the frequency response of the two matching networks was calculated in a more accurate way using a full wave electromagnetic solver based on the Method of Moments (MoM) technique. Figure 7 compares the behavior of the amplifier obtained with the circuital model and with the MoM technique, predicting that the frequency response of the manufactured prototype, which is expected to be similar to that obtained with MoM, will appreciably degrade, reducing the bandwidth and the gain. Thus, the impedance matching networks have to be modified in order to achieve that their MoM frequency response match that obtained with the circuital model after the two step optimization and, hence, leading to the desired behavior of the implemented prototype. To do that, an easily implementable procedure, specially suited to the NUTL characteristics, was developed. Taking the circuital implementation of the NUTL as reference, its actual nominal length $L = L_{nom}$ is modified until its frequency response is as close as possible to that obtained with the MoM technique. Let us assume that the necessary length modification is δl and, hence, the length after this step is $L' = L_{nom} + \delta l$. Next, a new NUTL schematic model is created, with length $L'' = L_{nom} - \delta l$, keeping constant all the width parameters. If the value of δl is small enough, which occurs when the circuital model is acceptable, the MoM frequency response of the new structure will match that of the original circuital model. Since the calculation of the correction factor δl is performed over the circuital model, a reiterative rescaling of the electromagnetic model (MoM) is avoided, which results in a reduction of design time. The frequency

response of the amplifier after the correction is superimposed in Fig. 7, showing the validity of the proposed correction method, because of the agreement between the corrected electromagnetic and the initial circuital models. Finally, the value of $\Gamma_{in,f}$, evaluated before and after the correction, is represented in Fig. 8. From the similarity between the two traces, it can be concluded that the noise figure of the of the amplifier will not be appreciably degraded.

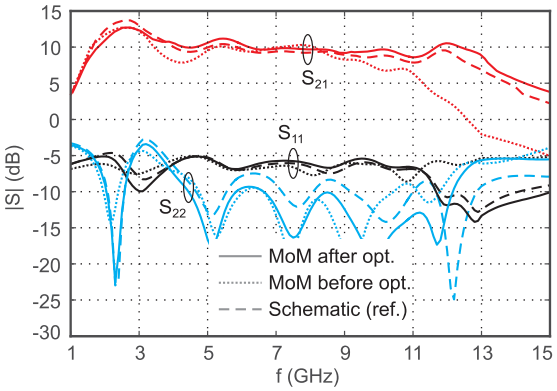

FIGURE 7. Influence of the electromagnetic effects that are not taken into account in circuital models on the circuit performance, and frequency response of the amplifier after correcting the impedance matching networks.

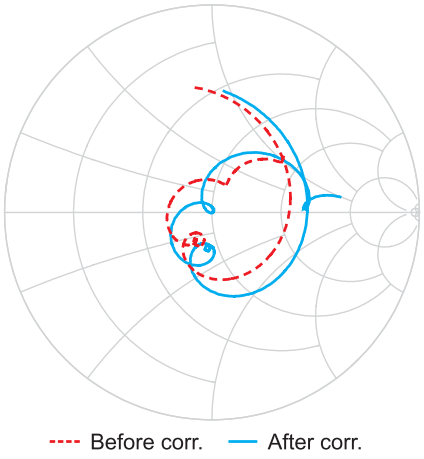

FIGURE 8. $\Gamma_{in,f}$ before and after the fine tuning of the matching networks.

IV. IMPLEMENTATION

A prototype was implemented on *Arlon 25N* substrate, with nominal dielectric constant $\varepsilon_r = 3.38$, $tan\delta = 0.0025$, and thickness $h = 0.75$ mm. This substrate was selected because it provides a good trade-off between cost and variation of losses with frequency, and due to its mechanical rigidity. The circuit was structured through a laser ablation procedure, which is able to accurately reproduce the shape of the optimized matching networks. Two end-launch SMA connectors, with maximum working frequency $f_{max} = 27$ GHz, from *Southwest Microwave* were used as coaxial interface with the measurement equipment. A picture of the implemented prototype is shown in Fig. 9.

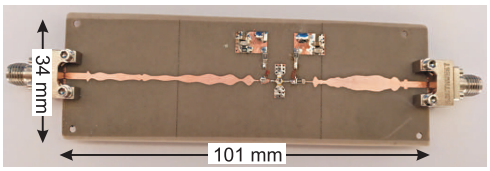

FIGURE 9. Implemented prototype. Left hand side connector corresponds to input port.

The RF chokes used as a part of the DC-bias networks were in-house implemented as air core coils, with 0.55 mm core diameter, 0.02 mm wire diameter and 7.5 turns, which provides an inductance value $L_{\text{choke}} \approx 12$ nH and estimated self resonance frequency, f_{SRF}, above 14 GHz [32], when mounted on the circuit.

V. EXPERIMENTAL RESULTS

The implemented prototype was characterized in terms of its frequency response, noise figure and linearity.

A. FREQUENCY RESPONSE

The S parameters of the amplifier were directly measured through a *Keysight N5247A PNA-X* Vector Network Analyzer (VNA). They are represented in Fig. 10, together with simulation data obtained when considering the MoM evaluated frequency response of the corrected matching networks. The measured bandwidth is slightly reduced when compared with simulation data, which could be due to a reduction of the particular f_{SRF} value of the RF chokes, which depends on the way they are mounted. At any case, the prototype provides a nearly flat frequency response with 10 dB gain between 1 and 12 GHz, $S_{11} < -6$ dB, and $S_{22} < -10$ dB over most of the considered range. The good agreement between simulation and measurement results demonstrates the potential of the impedance matching networks based on

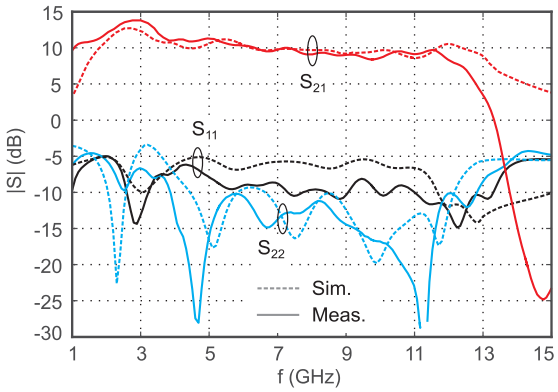

FIGURE 10. Measured frequency response of the implemented prototype, compared with simulation data. Continuous traces represent experimental data. Dashed lines correspond to simulation data.

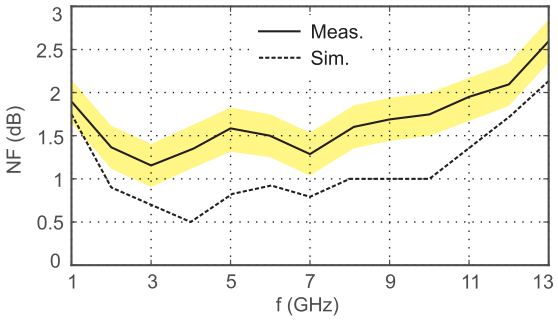

FIGURE 11. Measured Noise Figure, compared with simulation data. The shaded area represent the measurement uncertainty $\sigma = \pm 0.25$ dB.

non-uniform transmission lines, and the validity of the design methodology.

B. NOISE FIGURE

The amplifier noise figure NF was measured using the Y-factor method [33]. A *Rohde&Schwartz FSP40* spectrum analyzer was used as measurement instrument, together with the noise source *NC346A*, from *NoiseCom*. Since the available spectrum analyzer has not a built-in preamplifier, an external one was used to improve the measurement accuracy. The selected model is the *Herotek A182275*. The obtained results are depicted in Fig. 11, together with simulation data. The measurement uncertainty σ was determined from the previously measured values of gain and input and output matching (see Fig. 10), and the noise source parameters provided by the manufacturer. It was found to be $\sigma = \pm 0.25$ dB in the worst case. Simulation data was obtained by comparing the reflection coefficient $\Gamma_{in,f}$ with the theoretical noise circles. Note that the values of $\Gamma_{in,f}$ obtained through electromagnetic simulation have to be used in order to ensure accurate results.

C. LINEARITY

The amplifier linearity was characterized through the measurement of the well known figures of merit 1 dB compression point, P_{1dB}, and the Third Order Interception Point OIP3. The obtained results are represented in Fig. 12, together with simulation data, showing good agreement between them. The measured values of P_{1dB} and OIP3 are consistent with the topology of the amplifier, which uses only one small signal transistor, with the transistor characteristics provided by the manufacturer, and with the DC-bias point. The P_{1dB} reduction observed at $f = 2$ GHz is due to the peak gain achieved around that frequency. In the case of the OIP3, it is a classical figure of merit that is only able to provide a rough idea about the circuit linearity. To characterize it in a more complete way, the output power difference between the fundamental and the third order distortion components, $\Delta P = P_{fund} - P_{3rd}$, was measured, for different values of input power P_{in}. The frequency separation between the two test tones was selected to be 10 MHz. The result is represented in Fig. 13, showing that, when the input power is around 5 dB smaller than P_{1dB}, the power difference between the fundamental component and the third order distortion one is bigger than 40 dB over most of the considered frequency range.

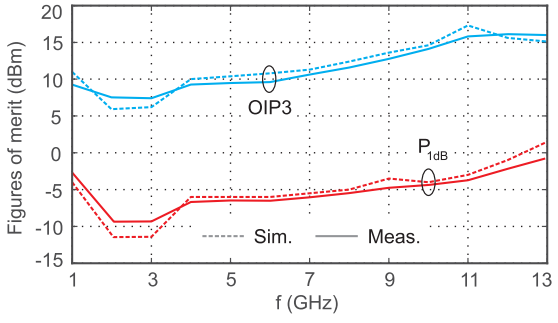

FIGURE 12. Comparison between simulated and measured figures of merit P_{1dB} and OIP3.

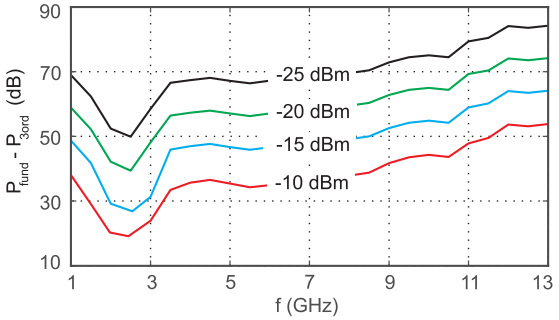

FIGURE 13. Measured power difference $\Delta P = P_{fund} - P_{3rd}$ between the fundamental and the third order distortion components, for different input signal levels.

Finally, in order to provide a general overview of the described design approach capabilities, and the LNA performance, two comparisons with previously published works were performed. First, Table 1 summarizes a performance comparison between the prototype presented in this work and other LNAs recently reported. From the table, the prototype presented in this work provides competitive results in terms of broadband low-noise amplification in the low microwave band. Note that, in this work, the amplifier is implemented in hybrid technology using a single encapsulated GaAs pHEMT transistor, whereas the cited works present MMIC implementations based on feedback transistors. Furthermore, the references marked with (*) describe CMOS devices composed of

TABLE 1. Performance comparison between LNAs.

Ref.	BW (GHz)	BW (%)	Gain (dB)	NF (dB)	S_{11}, S_{22} (dB)
[1](*)	2.3-9.2	120	10	4 (min.)	$< -10, < -10$
[2](*)	3.1-10.6	109	15	2.5 ± 0.25	< -9.9, n.a.
[3](*)	2.4-5.4	77	22	2.2-3.1	< -12, n.a.
[4](*)	3.1-10.6	109	11	4.5-5	< -11, n.a.
[5](**)	11-39	112	23	2.1-3	$< -2, < -10$
[6](**)	18-43	82	21.6	1.8-2.7	$< -5, < -9$
[7](**)	3.7-10.5	96	12	1.4-2	$< -9, < -9$
This work	1-12.5	170	10	2.25 (max.)	$< -5, < -5$

TABLE 2. Performance comparison between PAs.

Ref.	BW (GHz)	BW (%)	Gain (dB)	S_{11}, S_{22} (dB)	Size (mm^2) $L \times W$
[8]	1.3-3.3	86	10	n.a.	60×43
[9]	1.45-2.45	51	10	n.a.	$103\times$ n.a.
[10]	0.9-3.2	112	10-14	n.a.	n.a.
[11]	1.7-2.6	42	10.2-11.6	n.a.	n.a.
[13]	0.2-1.8	160	12-15	n.a.	75×58
[14]	0.3-8	185	8.5	< -5	n.a.
This work	1-12.5	170	10	< -5	101×34

one amplifier stage and an output buffer, and the references marked with (**) are relative to multistage GaAs pHEMT devices. On the other hand, since broadband LNAs implemented in hybrid technology using a single encapsulated transistor are not commonly found, the prototype was also compared with some broadband power amplifiers with the cited characteristics, in order to demonstrate the potential of the proposed approach in terms of the ratio size *vs.* bandwidth. Power amplifiers with lowest frequency limit similar to that of the actual prototype were selected, since this factor strongly conditions the size of the matching networks. The results are shown in Table 2. In this case, the comparison was performed in terms of the working frequency, the bandwidth and the device size, whereas parameters relative to the output power and efficiency were not taken into account. From the table, the proposed approach is able to provide large relative bandwidth when considering similar lowest frequency limit, while maintaining moderate circuit size.

VI. CONCLUSION

The viability of a new approach for the design of custom broadband amplifiers in hybrid technology based on the use of Non-Uniform Transmission Lines (NUTL) as practical wide-band impedance matching networks has been demonstrated. Furthermore, the synthesis of the NUTL shape taking advantage of the optimization tools integrated in CAD packages, combined with the inherent flexibility of the NUTL structures, allows the development of a systematic and fast design procedure which is easily implementable in most CAD packages, and avoids the use of additional external algorithms. To illustrate the technique, it was applied to the design of a broadband low noise amplifier but, due to its versatility, it can be easily extrapolated to the design of broadband power or multi-stage amplifiers. A prototype was manufactured and experimentally characterized, simultaneously providing a 10 dB gain flat frequency response, noise figure less than 2 dB, and acceptable input and output impedance matching between 1 and 12 GHz, which is in good agreement with simulation data.

REFERENCES

[1] A. Bevilacqua and A. M. Niknejad, "An ultrawideband CMOS low-noise amplifier for 3.1–10.6-GHz wireless receivers," *IEEE J. Solid-State Circuits*, vol. 39, no. 12, pp. 2259–2268, Dec. 2004.

[2] M. T. Reiha and J. R. Long, "A 1.2 V reactive-feedback 3.1-10.6 GHz low-noise amplifier in 0.13 *u*m CMOS," *IEEE J. Solid-State Circuits*, vol. 42, no. 5, pp. 1023–1033, May 2007.

[3] C.-T. Fu, C.-L. Ko, C.-N. Kuo, and Y.-Z. Juang, "A 2.4–5.4-GHz wide tuning-range CMOS reconfigurable low-noise amplifier," *IEEE Trans. Microw. Theory Techn.*, vol. 56, no. 12, pp. 2754–2763, Dec. 2008.

[4] C.-T. Fu, C.-N. Kuo, and S. S. Taylor, "Low-noise amplifier design with dual reactive feedback for broadband simultaneous noise and impedance matching," *IEEE Trans. Microw. Theory Techn.*, vol. 58, no. 4, pp. 795–806, Apr. 2010.

[5] G. Nikandish and A. Medi, "Transformer-feedback interstage bandwidth enhancement for MMIC multistage amplifiers," *IEEE Trans. Microw. Theory Techn.*, vol. 63, no. 2, pp. 441–448, Feb. 2015.

[6] G. Nikandish, A. Yousefi, and M. Kalantari, "A broadband multistage LNA with bandwidth and linearity enhancement," *IEEE Microw. Wireless Compon. Lett.*, vol. 26, no. 10, pp. 834–836, Oct. 2016.

[7] Y.-C. Hsiao, C. Meng, and M.-C. Li, "Analysis and design of BroadbandLC-Ladder FET LNAs using noise match network," *IEEE Trans. Microw. Theory Techn.*, vol. 66, no. 2, pp. 987–1001, Feb. 2018.

[8] K. Chen and D. Peroulis, "Design of broadband highly efficient harmonic-tuned power amplifier using in-band continuous class-F^{-1}/F mode transferring," *IEEE Trans. Microw. Theory Techn.*, vol. 60, no. 12, pp. 4107–4116, Dec. 2012.

[9] N. Tuffy, L. Guan, A. Zhu, and T. J. Brazil, "A simplified broadband design methodology for linearized high-efficiency continuous Class-F power amplifiers," *IEEE Trans. Microw. Theory Techn.*, vol. 60, no. 6, pp. 1952–1963, Jun. 2012.

[10] Z. Dai, S. He, F. You, J. Peng, P. Chen, and L. Dong, "A new distributed parameter broadband matching method for power amplifier via real frequency technique," *IEEE Trans. Microw. Theory Techn.*, vol. 63, no. 2, pp. 449–458, Feb. 2015.

[11] J. Pang, S. He, C. Huang, Z. Dai, J. Peng, and F. You, "A post-matching Doherty power amplifier employing low-order impedance inverters for broadband applications," *IEEE Trans. Microw. Theory Techn.*, vol. 63, no. 12, pp. 4061–4071, Dec. 2015.

[12] P. Chen, B. M. Merrick, and T. J. Brazil, "Bayesian optimization for broadband high-efficiency power amplifier designs," *IEEE Trans. Microw. Theory Techn.*, vol. 63, no. 12, pp. 4263–4272, Dec. 2015.

[13] Y. Zhuang, Z. Fei, A. Chen, Y. Huang, and K. Rabbi, "Design of multioctave high-efficiency power amplifiers using stochastic reduced order models," *IEEE Trans. Microw. Theory Techn.*, vol. 66, no. 2, pp. 1015–1023, Feb. 2018.

[14] A. Sayed, S. Preis, and G. Boeck, "Efficient technique for ultra broadband, linear power amplifier design," *Int. J. Microw. Wireless Technol.*, vol. 4, no. 6, pp. 559–567, Aug. 2012.

[15] T. Lopetegi *et al.*, "New microstrip 'Wiggly-Line' filters with spurious passband suppression," *IEEE Trans. Microw. Theory Techn.*, vol. 49, no. 9, pp. 1593–1598, Sep. 2001.

[16] G. Xiao and K. Yashiro, "Impedance matching for complex loads through nonuniform transmission lines," *IEEE Trans. Microw. Theory Techn.*, vol. 50, no. 6, pp. 1520–1525, Jun. 2002.

[17] Y.-W. Hsu and E. F. Kuester, "Direct synthesis of passband impedance matching with nonuniform transmission lines," *IEEE Trans. Microw. Theory Techn.*, vol. 58, no. 4, pp. 1012–1021, Apr. 2010.

[18] I. Arnedo, M. A. G. Laso, F. Falcone, D. Benito, and T. Lopetegi, "A series solution for the single-mode synthesis problem based on the coupled-mode theory," *IEEE Trans. Microw. Theory Techn.*, vol. 56, no. 2, pp. 457–466, Feb. 2008.

[19] I. Arnedo *et al.*, "Synthesis of one dimensional electromagnetic bandgap structures with fully controlled parameters," *IEEE Trans. Microw. Theory Techn.*, vol. 65, no. 9, pp. 3123–3134, Sep. 2017.

[20] I. Arnedo, J. D. Schwartz, M. A. G. Laso, T. Lopetegi, D. V. Plant, and J. Azana, "Passive microwave planar circuitsfor arbitrary UWB pulse shaping," *IEEE Microw. Compon. Lett.*, vol. 18, no. 7, pp. 452–454, Jul. 2008.

[21] A. Santorelli *et al.*, "Experimental demonstration of pulse shaping for time-domain microwave breast imaging," *Prog. Electromagn. Res.*, vol. 133, pp. 309–329, Oct. 2013.

[22] S. Ver-Hoeye *et al.*, "Multi-harmonic DC-bias network based on arbitrarily width modulated microstrip line," *Prog. Electromagn. Res. Lett.*, vol. 11, pp. 119–128, 2009. doi: doi:10.2528/PIERL09071605.

[23] G. Hotopan, S. V. Hoeye, C. Vázquez, R. Camblor, M. Fernández, and F. L. Heras, "Multi-harmonic submillimeter-wave dc-bias network based on an arbitrarily width-modulated microstrip line," in *Proc. 40th Eur. Microw. Conf.*, Sep. 2010, pp. 1365–1368.
[24] M. Fernandez-Garcia, S. Ver-Hoeye, C. Vazquez-Antuna, G. R. Hotopan, R. Camblor-Diaz, and F. L. H. Andres, "New non-linear approach for the evaluation of the linearity of high gain harmonic self oscillating mixers," *Prog. Electromagn. Res.*, vol. 126, pp. 149–168, Mar. 2012.
[25] S. V. Hoeye, M. G. Corredoiras, M. F. Garcia, C. V. Antuna, L. F. H. Ontanon, and F. L. H. Andres, "Harmonic Optimization of Rationally Synchronized Oscillators," *IEEE Microw. Wireless Compon. Lett.*, vol. 19, no. 5, pp. 317–319, May 2009.
[26] M. Fernandez-Garcia, S. Ver-Hoeye, C. Vazquez-Antuna, G. R. Hotopan, R. Camblor-Diaz, and F. L. H. Andres, "Optimization of the synchronization bandwidth of rationally synchronized oscillators based on bifurcation control," *Prog. Electromagn. Res.*, vol. 119, pp. 299–313, Aug. 2011.
[27] M. Fernandez-Garcia, S. Ver-Hoeye, C. Vazquez-Antuna, G. R. Hotopan, R. Camblor-Diaz, and F. L. H. Andres, "Non linear optimization technique for the reduction of the frequency scanning effect in a phased array based on broadband injection-locked third harmonic self-oscillating mixers," *Prog. Electromagn. Res.*, vol. 127, pp. 479–499, May 2012.
[28] M. Fernandez-Garcia, S. Ver-Hoeye, C. Vazquez-Antuna, G. R. Hotopan, R. Camblor-Diaz, and F. L. H. Andres, "Analysis of the locking range of rationally synchronized oscillators with high reference signal power," *IEEE Trans. Microw. Theory Techn.*, vol. 60, no. 8, pp. 2494–2504, Aug. 2012.
[29] M. González *et al.*, "Non-linear optimization of an injection locked high efficiency VCO with arbitrarily width modulated microstrip line networks," *Prog. Electromagn. Res.*, vol. 140, pp. 491–508, Jun. 2013.
[30] M. González *et al.*, "Non-linear design, optimization and analysis of an injection-locked high efficiency VCO with arbitrarily width modulated microstrip line networks," in *Proc. IEEE Int. Telecommun. Symp.*, Aug. 2014, pp. 1–5.
[31] G. González, *Microwave Transistor Amplifiers*, 2nd ed. Upper Saddle River, NJ, USA: Prentice-Hall, 1997, ch. 3, pp. 257–272.
[32] B. S. Virdee, A. S. Virdee, and B. Y. Banyamin, *Broadband Microwave Amplifiers*, 2nd ed. Norwood, MA, USA: Artech House, 2004, ch. 7, pp. 185–187.
[33] M. Leffel and R. Daniel. *The Y Factor Technique for Noise Figure Measurement*. Accessed: Feb. 07, 2019. [Online]. Available: https://scdn.rohde-schwarz.com/ur/pws/dl_downloads/dl_application/application_notes/1ma178/1MA178_3e_NoiseFigure.pdf

MIGUEL FERNÁNDEZ received the M.Sc. degree in telecommunication engineering, the M.Sc. degree in information technology and mobile communications, and the Ph.D. degree from the University of Oviedo, Gijón, Spain, in 2006, 2010, and 2010, respectively.

From 2006 to 2008, he was a Research Fellow with the Signal Theory and Communications Group, University of Oviedo, where he has been an Associate Professor, since 2008. His main research effort is focused on nonlinear analysis and optimization techniques for the design of oscillator-based circuits, active antennas, and frequency multipliers and mixers at the microwave, millimeter/submillimeter-wave, and terahertz frequency bands.

SAMUEL VER HOEYE (M'05) received the M.Sc. degree in electronics engineering from the University of Ghent, Ghent, Belgium, in 1999, and the Ph.D. degree from the University of Cantabria, Santander, Spain, in 2002.

He is currently an Associate Professor with the Department of Electrical and Electronic Engineering, University of Oviedo, Gijón, Spain. His main research is focused on the design and analysis of microwave, millimeter-wave, and terahertz circuits and systems. Among these are the multi-functional oscillator-based circuits and antennas, frequency scanning antennas, graphene-based frequency multipliers and mixers, imaging systems, and textile integrated high-frequency components.

CARLOS VÁZQUEZ received the M.Sc. degree in telecommunication engineering, the M.Sc. degree in information technology and mobile communications, and the Ph.D. degree from the University of Oviedo, Gijón, Spain, in 2007, 2008, and 2013, respectively.

From 2007 to 2012, he was a Graduate Research Assistant with the Signal Theory and Communications Group, University of Oviedo, where he has been a Research Fellow, since 2012. His research efforts mainly focus on nonlinear analysis and optimization techniques for the design of multifunctional oscillator-based circuits, active antennas, and passive components, such as frequency multipliers and harmonic mixers, at microwave, millimeter/submillimeter-wave, and terahertz frequencies.

LETICIA ALONSO received the M.Sc. degree in telecommunication engineering from the University of Oviedo, Gijón, Spain, in 2014, the M.Sc. degree in systems and control engineering from the National University of Distance Learning and the Universidad Complutense de Madrid, Spain, in 2018, and the Ph.D. degree from the University of Oviedo, in 2018.

She was a Visiting Scholar with the George Green Institute for Electromagnetics Research, University of Nottingham, U.K., in 2017. Since 2014, she has been a Researcher with the Signal Theory and Communications Group, University of Oviedo. Her main research effort is focused on the design, simulation, and manufacturing techniques to develop microwave and millimeter-wave passive circuits and antennas fully integrated in textile technology.

FERNANDO LAS-HERAS received the M.S. degree and the Ph.D. degree in telecommunication engineering from the Tech University of Madrid (UPM), in 1987 and 1990, respectively. From 1988 to 1990, he was a National Graduate Research Fellow. From 1991 to 2000, he was an Associate Professor with the Department of Signal, Systems and Radiocom, UPM. From 2004 to 2008, he was the Vice-Dean for Telecommunication Engineering with the Tech School of Engineering, Gijón. He was a Visiting Researcher with Syracuse University, NY, USA, and a Visiting Lecturer with the National University of Engineering, Lima, and ESIGELEC, France. From 2005 to 2015, he held the Telefónica Chair (on RF technologies, ICTs applied to environment and climate change, and ICTs and smartcities). He has been the Head of the Research Group Signal Theory and Communications (TSC-UNIOVI), Department of Electrical Engineering, University of Oviedo, since 2001. He has been a Full Professor with the University of Oviedo, since 2003. He has authored over 450 technical journal and conference papers in the areas of electromagnetic radiation, propagation, and scattering theory and applications as well as inverse problems. He was a member of the Board of Directors of the IEEE Spain Section, from 2012 to 2015, a member of the Board of the IEEE Microwaves and Antennas Propagation Chapter (AP03/MTT17), from 2016 to 2018, and a member of the Science, Technology and Innovation Council of Asturias, Spain, in 2010.